Improvement of Resistance Spot Welding by Surfaces Treatment of AA1050 Sheets

Dr. Qasim Mohammed Doos Al-Attaby
Professor
Mechanical Engineering
Baghdad University
Kasim_daws@yahoo.com

Dr. Moneer Hammed Al Saadi
Assistance Professor
Welding Department
Technical College-Baghdad
monerht@yahoo.com

Ihsan Kadhom Abbas Al Naimi
Ph.D.
Mechanical Engineering
Baghdad University
Ihsan_kad@yahoo.com

ABSTRACT

Resistance spot welding (RSW) aluminum alloys has a major problem of inconsistent quality from weld to weld, because of the problems of the non-uniform oxide layer. The high resistivity of the oxide causes strong heat released which influence significantly on the electrode lifetime and the weld quality. Much effort has been devoted experimentally to the study of the sheet surface characteristics for as-received sheet and surface pretreatment sheet by pickling in NaOH and glass-blasted with three thicknesses (0.6, 1.0, and 1.5 mm) of AA1050. Three different welding process parameters energy setup as a low, medium, and high were carried. Tensile-shear strength tests were performed to indicate the weld quality. Moreover, microhardness tests, macro/micrographs, and SEM/EDS examinations were carried out to analyze, compare, and evaluate the effect of surface conditions on the weldability. The as-received sheet showed a higher electrical contact resistance because of its thicker and non-uniform oxide layer. In contrast, the glass-blasted sheet showed lower value, since it has a roughest surface, which leads to easy breakdown the oxide layer. The highest average values and least scattering of the maximum load fracture are with treated sheet by pickling in NaOH, these values are 760, 1193, and 2283 N for 0.6, 1.0, and 1.5 mm sheet thickness respectively for medium input energy. In contrast, the minimum values with glass-blasted sheet are 616, 1008, and 2020 N for 0.6, 1.0, and 1.5 mm sheet. The microhardness profiles of the fusion zone and HAZ is the lower than the base metal for all cases. Numerical simulation with SORPAS® was used to simulate and optimize the process parameters, and it has given good results in prediction when they compared with experiments.

Keywords: RSW Oxide Film Roughness Macro/Micrograph SEM/EDS AA1050 SORPAS®

تحسين لحام المقاومة النقطي بمعالجة أسطح صفائح سبيكة الالومنيوم AA1050

أ. د. قاسم محمد دوس العتابي أ. م. د. منير حميد طلفيح السعدي إحسان كاظم عباس النعيمي

الخلاصة

لحام المقاومة النقطي لسبائك الالمونيوم يتضمن مشكلة كبيرة في استقرارية جودة اللحام من لحام إلى لحام آخر بسبب عدم انتظام سمك طبقة الاوكسيد. المقاومة الكهربائية العالية لطبقة الاوكسيد تسبب في توليد حرارة عالية، والتي لها تأثير كبير على العمر التشغيلي للاقطاب وجودة اللحام. كُرس جهد كبير عملياً لدراسة خصائص سطح الصفائح الغير معالجة وتلك المعالجة كيميائياً بهيدروكسيد الصوديوم وبالقصف بالكرات الزجاجية ولثلاثة أسماك (0.6 ، 1.0 ، و 1.5 ملم) لصفائح سبيكة AA1050 وقد تم إجراء ثلاثة إعدادات مختلفة لمدخلات طاقة اللحام منخفض، متوسط، ومدخلات الطاقة العالية. قوة اللحام تم تقييمها بفحص الشد- القص. فضلاً عن ذلك، تم إجراء فحص الصلادة الدقيقة، الصور الماوغرافية والمايكروية، والماسح الالكتروني مع التحليل الطيفي بهدف المقارنة وتقييم تأثير حالة السطح على جودة اللحام. الصفائح كما جهزت (الغير معالجة) أظهرت مقاومة تماس كهربائية عالية بسبب السماكة الاكثر والغير منتظمة لطبقة الاوكسيد. وعلى النقيض، الصفائح المعالجة بالقصف بالكرات الزجاجية أظهرت أقل قيمة، حيث لها سطح خشن الذي يساعد على تكسر طبقة الاوكسيد بسهولة. أعلى قوة ملحومات مع أقل تشتت حصلت مع الصفائح المعالجة بهيدروكسيد الصوديوم هذه القيم هي 760، 1193، 2283 نيوتن للصفائح سمك 0.6، 1.0، 1.5 ملم على التوالي. على النقيض، أقل قيم لقوة الملحومات مع الصفائح المعالجة بالقصف بالكرات الزجاجية وهي 616، 1008، 2020 نيوتن للصفائح سمك 0.6، 1.0، 1.5 ملم على التوالي. منحني الصلادة الدقيقة لمنطقة الانصهار والمنطقة المتأثرة بالحرارة هي أقل من المعدن الاساس ولكل حالات الصفائح. تم استخدام المحاكاة العددية مع برنامج SORPAS® لمحاكاة وتمثيل متغيرات عملية اللحام، وأعطى تنبؤ جيد عند المقارنة مع التجارب العملية.

الكلمات الرئيسية : لحام المقاومة النقطي طبقة الاوكسيد خشونة السطح صور ماوغرافية ومايكروية الماسح الالكتروني

INTRODUCTION

Todays, World is faced with an energy crisis. It is therefore essential to find cost-effective solutions to this issue. Therefore, there has been a significant trend in the automobile industry by economic and political pressure to make lighter vehicles in order to reduce fuel consumption and CO_2 emission. Because of their lightweight and high specific strength (strength-to-weight ratio), the application of aluminum alloys in automobile industry is being increased and popularity. The advantages of weight saving up to 46% [Wheeler, 1987] and resistance of corrosion are considerable.

Resistance Spot Welding (RSW) has been the dominant process in sheet metal joining, particularly in automobile industry. Because of its low cost, flexible, easy automated and maintains, fast, and minimum skill labor requirements. Moreover, it is a well-established process in the automotive industry [Brown, 1995 and Cho, 2006]. The process is also applied in manufacture of other transportation, kitchen utensils, and more. Modern small vehicles contain (2000-5000) spot welds [Chao, 2003]. Annual production of automobiles in the world is measured in tens of millions units; therefore, each welded spot has its own importance not only with regard to quality but also for production issue. Steel and aluminum alloys share many of the same process attributes for RSW. However, the productivity of aluminum spot welding is lower than of steel especially those alloys with low strength (series 1xxx). This is because aluminum alloys have higher thermal and electrical conductivity, higher coefficient of expansion, narrow plastic temperature range, and oxide film problems, which forms on the surface of the aluminum and has high electrical resistance and a high melting temperature (2050℃), as the oxide film grows the effective contact resistance of the aluminum changes. Therefore, the control of weld quality is much more difficult and requires tighter controls [Kim, 2009]. In general, aluminum's high thermal and electrical conductivity require higher current, shorter weld time, about (2-3) times the amount of current and (¼) weld time compared to spot welding steel. Accurate control and synchronization of current and electrode force is required due to the narrow plastic temperature range [RWMA, 2003]. Aluminum is highly reactive to oxygen and will within 100 picoseconds form thin protective oxide layer (Al_2O_3) on its surface and is often considered be a uniform ceramic coating or layer. This layer is beneficial as it protects the base metal from corrosion. While this may be close to reality for high-purity aluminum, the oxide layer on the aluminum alloy sheets for automotive bodies is much more complex [Patrick, 1984]. The oxide layer is important because its thickness is an influential parameter in the electrical resistance [Sun, 1982]. The high resistivity of the oxides causes strong heat release. Fusion of the low melting alloy takes place not only at the sheet-to-sheet interfaces but also at the sheet-to-electrode contacts, resulting in unacceptable electrode wear.

RSW is a welding process that joint sheet metal together by applying pressure and passing a large quantity of current through localized area generating heat by Joule ohmic heating law while weld nugget growth is initiated here and the sheets are permanently fixed together. Thereby, electrical contact resistance is one of the most critical parameters in resistance welding. A large contact resistance is advantageous for the formation of a single spot weld. As discussed by Browne, et al. [Browne, 1995] contact resistance plays an important role in the RSW process for aluminum. It has drawn the attention of many researchers since several decades ago, [Studer, 1939] carried out many experiments to demonstrate the influences of the pressure, temperature, and materials and its state on the contact resistance. With assistance of Gleeble system, contact resistance was experimentally investigated dynamically by [Song, 2005]. They demonstrated that interface normal pressure has great influence on the contact resistance and it decreases with increased normal pressure, in contrast, the influence of temperature on contact resistance is less pronounced as pressure increases.

Surface roughness along with elastic-plastic properties of the materials; also influence the electrical contact resistance [Dzekster, 1990]. The effect of surface roughness and oxide film thickness on the electrical contact resistance of aluminum were carried out by [Crinon, 1997], they illustrated

That the effect of the oxide film is greatest in the specimen with smoothest surfaces.

Expulsion, which can be observed frequently during RSW, happens at either the faying surface or

the electrode/work piece interfaces. The latter may severely affect surface quality and electrode life. The risk of expulsion is especially high in spot welding of aluminum alloys due to the very dynamic and unstable character of the process, relating to the application of a high current in a short welding time as compared to welding steels [Senkara, 2004 and Mathers, 2002].

RSW of aluminum alloys has two major problems: short electrode tip life and inconsistent weld quality [Williams, 1984]. Spot welding in AA1050 is less stable and the electrodes will stick to the sheet after 50 welds because of the oxide film problems [Pederson, 2010].

In this study, the influence of oxide film pretreatment on the strength of the weldments, which had done by RSW process was compared and evaluated. The pretreatment of the strips surfaces of AA1050 was done by both glass blast (mechanical mean) and pickling with NaOH (chemical mean).

EXPERIMENTAL PROCEDURE

The experiments were conducted at Technical University of Denmark (DTU), using 0.6, 1.0, and 1.5 mm sheet thicknesses of low-strength aluminum alloy AA1050, which were spot-welded on TECNA, the specifications of the welding machine are listed in **Table 1**. The Controller of the machine is TE-180 type with 16 functions. The electrode tips (Female Cap) used during the experiments are type A0 according to ISO 5821-2009, [RWMA, 2003]. They were made of Zirconium copper alloy with the following chemical compositions; Cr: 0.7-1.2%, Zr: 0.06-0.15% and the remainder is Cu. The configuration of them is radius type (A), diameter of 16 mm, end surface of 40 mm radius. The electrodes were drilled near the tips end with 1.5 mm diameter to insert copper wires in order to measure the secondary voltage. The current measurements from Rogowski coil together with a Pre-calibrated TECNA-1430 conditioner and a piezoelectric force sensor with Kistler-5015 transducer were acquired by a DAQ BNC-2110 from National Instruments and then passed to LabVIEW software programmer to treatment the signals .The properties and nominal compositions (performed by spectrum analyzer) of the sheets are shown in **Table 2**, the samples were cut from the sheets into 16 × 115 mm, the rolling direction with

the longitudinal dimension and they joined as a lap joining, to prepare the tensile-shear test. The parameters of the RSW process were calculated for each experiment, RMS current I (A), welding time C (cycle), and the electrode force P (kN). The tensile-shear tests were carried out using a 100 kN (22.5 kIb_f) AMSLER universal testing machine at a deformation rate 2mm/min at room temperature to demonstrate the strength of the weld S (N). The microhardness test were performed using FUTURE-TECH-CORP FM-700 using the Vickers scale at an applied load of 50 g, they were taken on each samples in longitudinal direction along the diameter of the nugget at intervals of 0.5 mm. The macro/micrographs of the weldments were carried out using light optical microscope (LOM) type a Neophot 30 (Zeiss, Jena) with a Cool Snap CCD camera. Moreover, for high-resolution images electron microscope (SEM) a JEOL JSM-5900 with LaB6 filament applying secondary electron (SE) at 20 kV, and electron-dispersion x-ray spectroscopy (EDS) part of a SEM facility an Oxford Instruments for quantitative chemical analysis were used.

The pretreatment of the surfaces of the strips were done by two methods: mechanical and chemical. The mechanical means was carried out by glass blast with grain size of 100 μm; each strip was subjected to 30 seconds of blast treatment at air pressure of 200 kPa. The experiments were done on both sides of the strips and other experiments were performed only on one side of the strips. The latter were welded with two directions; the pretreatment surfaces of the strips were the faying surfaces, and the alternative direction was the pretreatment surfaces with electrodes interface. The chemical means was done by pickling with sodium hydroxide (NaOH), the procedure of this approach was performed by sink the strips in solution 60 g of NaOH with one liter of ionized clean water within 2 minutes only, the temperature of the solution was

60℃. Then, the strips by hot water and ethanol were rinsed and cleaned for the both means to be ready for welding.

Aluminum is high affinity of oxygen, an oxide layer is always present at its surface and will immediately reform if surface pretreatment mechanically or chemically. For the stability of the oxide film, and repeating the experiments with the same conditions; the pretreatment strips were prepared within 3 hours before spot welding. This time was chosen depending on the **Fig. 1**, which was expected to have fresh, thin, and uniform oxide layer, while the as-received sheet would have thicker and non-uniform oxide layer.

The experiments were designed as a general factorial with three replicates per condition [Cho, 2006]. The factors and their associated parameters are given in **Table 3**. During welding, expulsion and sticking were observed and recorded.

RESULTS AND DISCUSSION

PICKLING IN NaOH

The electrical contact resistance at the interfaces sheet-to-sheet and sheet-to-electrode is the main source of heat during RSW of aluminum alloys, unlike steel, which the source of heat is the bulk resistance of the sheets. This electrical contact resistance depends strongly on the tribological characteristics of the contacts at the two interfaces. The significant factor impression tribological feature of aluminum sheets is the oxide layer. **Fig. 2** illustrates SEM image with EDS analyzer for as-received spot-welded strips, which show unambiguously the high amount of oxygen (3.6, 4.6, and 2.9%) near the area of strips separation. In the second importantly are the surface roughness and the presence of the foreign materials such as dirt, lubricant, chemical, water vapor, and others [Studer, 1939, Crinon, 1997, and Rashid, 2011]. Although of all care to maintain uniform surface conditions, the electrical contact resistance is almost different when another time measured in the same region. Therefore, the quality of RSW of aluminum alloys is inconsistent.

During pickling of aluminum alloy sheets in basic or acidic solutions the surface oxides or hydroxides are dissolved. The pickling rate is dependent on many variables including; 1- solution agent and concentration, 2- solution temperature, 3- composition of the surface sheet, 4- velocity of solution movement around the sheet (rpm). In earlier of this work, 5 minutes was chosen to sink the strips in the pickling agent (NaOH). However, it clearly seems that the corrosion rate of aluminum is much higher than the dissolution rate of the oxide layer. The formula of dissolution is:

$$Al_2O_3 + 2OH^- + 3\,H_2O \rightarrow 2Al(OH)_4^- \quad (1)$$

When the metal is bared; immediately corrodes according to this formula:

$$Al + 3H_2O + OH^- \rightarrow Al(OH)_4^- + \frac{3}{2}H_2 \quad (2)$$

The last formula shows that H_2 is evolved during dissolution of aluminum even in basic agent [Rö nhult, 1980]. Consequently, the metal is corroded by pitting as soon as the protecting layer of oxide film has been dissolved in some areas. Investigation by SEM shows strip exposure to NaOH within 5 minutes gave severe pitting corrosion of the surface, as shown in **Fig. 3**. Severe expulsions and sticking with electrodes were occurred during spot welding with these strips, due to the decreasing of electrical contact resistance in electrode sheet interface in spite of sheets interface especially with those of 0.6 mm strips. Therefore, all experiments latter were performed by exposure the strips to NaOH only within 2 minutes to minimize expulsion and sticking occurring.

SURFACE ROUGHNESS

Surface roughness measurements were carried out in this work on a Taylor/Hobson, Precision-SURTRONIC-25 instrument for various types of the strips to analyze and compare. Five measurements randomly on each of three strips for each surface condition and the average of all of them were recorded. **Table 4** shows these values of the centerline average (Ra) of as-received and pretreatment strips. It clearly seems that pretreatment sheets with glass blast show high values of roughness and the roughest surface is 1.0 mm sheet with glass blast (Ra = 4.703 µm), as seen

in **Fig. 4,** in contrast the smoothest surface is 1.5 mm as-received sheet (Ra = 0.238 μm). Chemical

Surface pretreatment (pickling in NaOH) shows the lowest value in standard deviation (s) when measured the surface roughness, and therefore it will be the most consistent in the weld strength. In contrast, the pretreatment strips with glass-blast show higher values in standard deviation although the attempt to control the removing surface layer precisely due to the manual process, and therefore it will be more scattering in welding strength as illustrated later.

The large variance between the smoothest and the roughest surfaces were clearly affected the strength of the weldments when were tested on the shear-tensile test. The glass-blasted strips show much lower contact resistance between sheet interfaces in spot welding causes less heat generated in this region, therefore small size nugget were produced, thus were affected the strength of the weldments. In the same sense, these strips show much lower sticking with electrodes, due to the lower heat generation since lower contact resistance in the region between sheet and electrode. Therefore, some experiments were conducted only on one side with glass-blast associated with sheet-to-electrode interface, and it shows as expected good weldability especially no sticking with electrodes and high strength with same process parameter.

Although there was a not high difference of roughness level between as-received and chemical treatment strips, there was a large difference in consistent of the welding quality between them. These results clearly demonstrate that the surface roughness is not the unique factor controlling the electrical contact resistance, but the oxide layer thickness and its configuration, which was similar to that found by other researchers [Patrick, 1984, Studer, 1939, Crinon, 1997, and Pouranvari, 2010]. It seems likely this result of surface roughness were associated with easier breaking down the oxide film in roughest surfaces when applying the electrode force during spot welding causes much lower contact resistance.

Fig. 5 shows LOM images, which confirm the variance of the surface roughness of the as-received sheet and the pretreatment sheet with pickling in NaOH and glass-blast.

TENSILE-SHEAR TESTS

Tensile-shear tests carried out on the welded joints indicated their strength and the failure mode. In this work, direct comparisons of the as-received surface with those of the pretreatment surface by pickling in NaOH and glass-blasted were established. **Fig. 6** shows the maximum fracture load for the spot welds as a function of welding input energy as mentioned in **Table 3** while other parameters are kept constant. The data point, which was represented in the figure, is the average of three specimens test. It is seen in general that with increasing energy input the maximum fracture load of spot welding increases. Moreover, the mode of failure is recorded and it is classified in three types; 1st interfacial failure (nugget fracture in shear), 2nd plug failure (nugget pull out), 3rd failure occurs in the heat affected zone (HAZ) where failure is a result of breaking this region throughout the width of the strip. The failure of spot welding could be seen as a competitive process, i.e. any failure occurs in a mode require least load [Newton, 1994]. These three types of the mode of failure were occurred usually as follows, the first type with low input energy, the second type with medium input energy, and finally the third type were occurred with high input energy for the three thicknesses sheets due to overheating and softening the region near the nugget perpendicular to strip width. A few anomalous specimens that have been observed during the testing did not fall under these types of failure. In line with other studies [Senkara, 2004, Mathers, 2002, and Ma, 2008], expulsion was occurred beyond the high input energy as well as of sever sticking sheet with electrodes. Furthermore, the fracture was usually in the form of ductile tearing around the nugget. Only a few weak welding failed in a brittle manner through the interface, and this was especially observed at low input energy.

The second observation, the scattering in maximum load fracture in tensile-shear tests is less in the pretreatment surfaces sheet with pickling in NaOH due to the new uniform less thickness of oxide layer. In addition, more scattering is with glass-blasted sheet due to the not good controlling manual process of removing the oxide layer. However, the maximum scattering values is with as-received sheet due to the non-uniform oxide layer,

which can scarcely be controlled without putting the samples in a vacuum.

The most important result obtained is that the average of maximum load fracture was the highest value in chemically treated with all thickness sheets. These values are 760, 1193, and 2283 N for 0.6, 1.0, and 1.5 mm sheet thickness respectively for medium input energy. In contrast, the minimum values of the maximum load fracture are in the glass-blasted sheet due to the lowest values of electrical contact resistance that lead in turn to be a small nugget size and thus small values of maximum load fracture. The electrical contact resistance of the roughest surface becomes lower value when electrode force is applied, due to the more breaking of the oxide layer, which is electrical insulating and this is a good agreement with many researchers as [Crinon, 1997]. These values are 616, 1008, and 2020 N for 0.6, 1.0, and 1.5 mm respectively. However, there is an interesting observation, which there is a significant increase in the maximum load fracture corresponding with glass-blasted treated strips on one side, which is the interface of the electrodes and the other faying surfaces remain untreated. The reason is higher heat generation due to higher electrical contact resistance at the faying surfaces and it is lower at the sheet-electrode interface and therefore less sticking with electrodes with increasing electrodes life. These values are 775, 1147, and 2408 N for 0.6, 1.0, and 1.5 mm sheet thickness respectively for the medium input energy.

MICROHARDNESS TESTS AND MICROSTRUCTURE EXAMINATIONS

Microhardness characteristics of the RSW are one of the most important factors affecting their failure behavior. Typically, the microhardness profile of the nugget of steel exhibit a significant hardness increase from the base metal due to the increasing of the martensite forming, and it is being more with alloy steel due to the content of alloying elements. An example of this behavior was recorded by [Hayat, 2011] with DP600 steel. With aluminum alloys, the microhardness values obtained from the fusion zone proved the existence of hard and brittle intermetallic phases due to the high content of the alloying elements thereby cause increasing of the hardness in that region. However, with low content of alloying elements as AA1050 the profile of microhardness is completely different, since the lower hardness is in the fusion zone. It is somewhat lower than the base metal, which can be attributed to its cast microstructure and the presence of coarse columnar grains. Moreover, the effect of the prior work hardening is completely removed in the fusion zone because of the melting.

Fig. 7 illustrates the variations of the microhardness profile for the pretreatment surfaces by mechanical (glass-blasted) and chemical (pickling in NaOH) and the as received of 1.0 mm sheets, which carried out on the cross section of the nugget to show the microhardness of the weld metals, HAZ region, and the base metals. The first important observation of profiles is that the microhardness of the fusion zone and HAZ is lower than the base metal for all cases, since these points were affected by the heat generated of welding, which were completely removed all previous work hardening especially in the fusion zone and its cast microstructure as mentioned above. The second observation, there are points with values of relatively low microhardness. These points are close to the voids defects result of the expulsion was occurred due to the high welding current (32 kA) for this sheet thickness, such as points 6 in glass-blasted sheet, point 7 in chemical pretreatment sheet, and point 5 in as-received sheet, which are observed in macrostructures were obtained by LOM. In contrast, there are a few points with relatively high values. Since, they are located on small grains and formed from intermetallic compounds, such as points 2, 2, and 8 in in glass-blasted, chemical pretreatment, and as-received sheet respectively, see the microstructures of these points as shown in **Fig. 7** (**a**), (**b**), and (**c**). Therefore, there is not a constant microhardness profile along the nugget.

In general, the microhardness measurements in fusion zone and HAZ of pretreatment surfaces with glass-blasted show highest values than the others, due to of the treatment by this means, which causes a few work hardening result of the hitting of the surface by glass grains during the oxide remover. In contrast, the microhardness measurements of as-received sheet show a lower values than the other pretreatment sheets due to the more heat generated at the faying surfaces since of the highest value of electrical contact resistance, as shown in **Fig 7** (**d**). Moreover, the microhardness of pretreatment

Surfaces by pickling in NaOH of the base metal show a lower value than the others due to the uniform fresh small thickness of oxide layer which consider as a harder material.

The macrographs show variations across the joints between the as-received sheets and the pretreatment surface sheets. The nugget size of the as-received weldments is larger than the pretreatment surfaces in the both means, since they are much lower contact resistance in the region of the faying surfaces, therefore lower heat generated. As an example, the nugget sizes are 5.1, 5.0, and 4.7 mm of 1.0 mm, 7.0, 6.54, and 5.35 mm of the 1.5 mm for as received, pickling in NaOH, and glass-blasted sheets respectively. The minimum size is with glass-blasted sheet that are less electrical contact resistance, which generates less heat.

The structures of aluminum weldments are usually not clearly distinguishable as in steel weldments, and the HAZ is significantly narrower for an aluminum weldments. These make the identification of various zones difficult. **Fig. 8** shows the micrographs of the 1.5 mm strips, which were welded with 32 kA welding current and 5 cycles welding time and the sheet were treated by pickling in NaOH. There are recrystallized small equiaxial grains and insoluble particles of $FeAl_3$ (black) in the oval nugget, and there are narrow zone of the columnar grains in the edge of the nugget and this zone is interfacial with the HAZ, which are formed of the dendritic grains. Moreover, some porosity (large, black area) is evident due to the splashes were occurred because of relatively high current was used. There are not a significant variation in the microstructures in the nugget and the HAZ of the weldments between the as received and the pretreatment sheets since the pretreatment is on the surfaces and not in the region which are heat affected. View of non-repetition, has not been discussed the microstructures of the other cases of the sheet condition that are not being a large variance from this case.

SEM AND EDS EXAMINATIONS

Further micrographs were carried out on SEM including secondary-electron images (SEI) to observe the nugget size, microstructures, surfaces profile, and together with X-ray spectroscopy (EDS) including high resolution mapping analyzing the chemical composition in the area of the interest. As-received sheet including non-uniform thick oxide layer caused indentation of the electrodes into the strips when spot-welded leading to degradation of the electrodes rapidly due to the pitting on the surface of the electrodes and dissolving or alloying the copper into the base metal of the aluminum or vice versa in this region. The reason of these problems is the high electrical resistance and a brittle nature of oxide layer causing relatively high heat generated in this region. The reason of few defects in the case of treated sheet might probably lie in the presence of the pitting on the electrodes surface because of the previous welding, as shown in **Fig. 9**.

The white color areas in the SEM images indicate the presence of the aluminum bronze with copper alloying element, as shown in the EDS analyzer table.

NUMERICAL SIMULATION

Commercial finite element numerical program SORPAS® [SWANTEC] was used in this work. It is well known and most widely used as a numerical tool for simulation, optimization, and planning features of the resistance welding processes. It is based on mechanical, electrical, thermal, and metallurgical models. In order to analyze and compare the experiments with the numerical modeling scheme, SORPAS® has been used to simulate a RSW of AA1050 with as-received sheet and the pretreatment sheet. Weld schedule specifications (WSS) is a new update input window included in the new version (10) of the program for optimized weld current, weld force, weld time, and hold time. **Table 5** indicates the WSS of the weld planning to optimize the RSW process parameters for as-received sheets. Furthermore, the process parameters for pretreatment sheets have been optimized in order to compare with as-received sheet. The value of electrical resistance at 20℃ in the materials database of the program was only changed to lower value, for the purpose of compatibility with oxide layer treatment. Only one result has changed that is the value of the welding current, which has become lower about 2 kA.

Fig. 10 shows the simulated joint for pretreatment by glass blast of 1.0 mm sheet

compared with experimentally macro etched cross-section nugget result welded with 29 kA welding current and 5 cycles welding time. It can be seen that the shape of the weld is predicted relatively a very fine correlation with the actual weld nugget, as well as the HAZ zone.

CONCLUSIONS

The experiments showed that weldability is improved when the oxide layer is properly removed. However, the resistance of an oxide layer is beneficial for the localized heating required to form the weld nugget, but this resistance should be as low as possible in order to minimize the heat generated at the interface between the electrodes and the sheets. The significant conclusions drawn from this experimental work are as follows:

1. The surface condition of aluminum sheet has a significant influence on the weldability and the electrode lifetime.
2. The optimum time immersing the strips in the solution of NaOH is 2 minutes at temperature of 60 °C.
3. In line with [Rashid, 2011] conclusions, the surface roughness affects the contact resistance by decreasing it where surface roughness increase, as it occurred with glass-blasted sheet, since it breakdown the oxide layer.
4. Treated sheet with pickling in NaOH gives highest average values of the maximum load fracture as shear-tensile test with all sheet thicknesses, as well as the scattering in the maximum load fracture is the least in this sheet, due to the fresh uniform oxide layer.
5. Less electrode sticking has occurred with one side surface treated that is electrode-sheet interface, in spite of good welding (maximum load fracture).
6. The microhardness profiles of the fusion zone and HAZ is the lower than the base metal for all cases where were completely removed all previous work hardening.
7. By examining macrographs of the welds, there are recrystallized small equiaxial grains and insoluble particles of $FeAl_3$ in the nugget and a narrow zone of columnar grains in the edge of it and this zone is interfacial with the HAZ, which are formed of dendritic grains.
8. SEM and EDS examinations confirm the presence of dissolving/alloying of the copper (electrode material) with aluminum (base sheet metal) in each other in as-received sheet more than the pretreatment sheet. Therefore, it is leading to degradation of the electrodes rapidly due to the pitting on the surface of the electrodes.
9. Numerical simulation with SORPAS® has given good results in predicted process parameters and the nugget size when they compared with experiments.

ACKNOWLEDGEMENT

This work is part of the cooperation between Baghdad University and DTU for independent research. The authors would like to thank Department of Mechanical Engineering at DTU, for helping with all practical work. Special thanks to Wenqi Zhang, director of SWANTEC for supplying the license of SORPAS® program. One author is grateful for the financial support by Iraqi Ministry of Higher Education and Scientific Research.

REFRENCES

Brown, D. J., Newton, C. J., and Boomer, D. Optimization and Validation of a Model to Predict the Spot Weldability Parameter lobes for Aluminum Automotive Body Sheet. Advanced Technologies & Processes, IBEC, pp. 100-106, 1995.

Browne, D. J., Chandler, H. W., Evans, J. T., and Wen, J. Computer Simulation of Resistance Spot Welding in aluminum, part one, Welding Journal 74(10), pp. 339-344, 1995.

Browne, D. J., Chandler, H. W., Evans, J. T., James, P. S., Wen, J., and Newton, C. J. Computer Simulation of Resistance Spot Welding in aluminum, part two, Welding Journal 74(12), pp. 417-422, 1995.

Chao, Y. J. Ultimate Strength and Failure Mechanism of RSW Subjected to Tensile, Shear, and combined tensile/Shear Loads. ASME journal of Engineering Materials and Technology, Vol. 125, 125-13, 2003.

Cho, W., Li, and Hu, Design of Experiment Analysis and Weld Lobe Estimation for Aluminum Resistance Spot Welding. Supplement to the Welding Journal, sponsored by the American

Welding Society and the Welding Research Council, 2006.

Crinon, E., Evans, J. T., The Effect of Surface Roughness, Oxide Film Thickness and Interfacial Sliding on the Electrical Contact Resistance of Aluminum. Material Science and Engineering Journal, A242, pp. 121-128, 1998.

Dzekster, N. N., and Ismailov, V. V. Some methods for Improving Aluminum Contacts. Proceeding of 36th Annual Holm conference on Electrical Contacts, Illinois Institute of Technology, Chicago III. pp. 518-520, 1990.

Hayat, F. The Effects of the Welding Current on Heat input, Nugget Geometry, and the Mechanical and fractural Properties of Resistance Spot Welding on Mg/Al Dissimilar Materials. Materials and Design, 32, 2476-2484, 2011.

Kim, D. C., Park, H. J., Hwang, I. S., Kang, M. J., RSW of Aluminum alloy sheet 5J32 Using SCR type and Inverter Type Power Supplies. International Scientific Journal, Vol. 38, Issue 1, Pages 55-60, 2009.

Ma, C., Chen, D. L., Bhole, S. D., Boudreau, G., Lee, A., Biro, E. Microstructure and Fracture Characteristics of Spot-Welded DP600 Steel. Materials Science and Engineering, 485, 334-346, 2008.

Mathers, G. The Welding of Aluminum and its alloys. Book published by Woodhead Publishing Limited, Cambridge CB1 6AH, England, 2002.

Newton, C. J., Browne, D. J., Thornton, M. C., Boober, D. R., and Keay, B. F. The Fundamental of Resistance Spot Welding Aluminum. Sheet Metal Conference VI, Paper E2, 1994.

Patrick, E. P., Auhl, J. R., and Sun, T. S. Understanding the Process Mechanism is Key to Reliable Resistance Spot Welding Aluminum Auto Body Components. SAE Technical Paper 840291, 1984.

Pederson, K. R. Resistance Welding of Aluminum Alloys. MSc. thesis, DTU, Department of Mechanical Engineering, Denmark, 2010.

Pouranvari, M. Prediction of Failure Mode in AISI 304 Resistance Spot Welds. Association of Metallurgical Engineers of Serbia, AMES, UDC: 621.791.763, PP. 23-29, 2010.

Rashid, M. Some Tribological Influences on the Electrode-Worksheet Interface during Resistance Spot Welding of Aluminum Alloys. Journal of Materials Engineering and Performance, Vol. 20(3), pp. 456-462, 2011.

RWMA, Resistance Welding Process. Resistance Welding Manuals, printed by George H. Buchman, Bridgeport, Nj USA, 2003.

R nhult, T., Rilby, U., and Olefjord, I. The Surface State and Weldability of Aluminum Alloys. Material Science and Engineering, 42, pp. 329-336, 1980.

Senkara, J., Zhang, H., and Hu, S. J., Expulsion Prediction in Resistance Spot Welding. Welding Research, Welding Journal, pp. 123-132, 2004.

Song, Q., Zhang, W., and Bay, N. An Experimental Study Determines the Electrical Contact Resistance in Resistance Welding. Sponsored by AWS and WRC, Welding Journal, pp. 73-76, 2005.

Studer, F. J. Contact Resistance in Spot Welding. Welding Journal, Vol.18, Iss. 10, pp. 374-380, 1939.

Sun, T. S. Electrode Deterioration Mechanisms in Resistance Spot Welding of Aluminum. Aloa Internal Report No. 53-82-3, 1982.

SWANTEC Software and Engineering ApS. SORPAS®, Version 10.6, www.swantec.com.

Wheeler, M. J., Sheasby, P. G., and Kewley, D. Aluminum Structured Vehicle Technology. A comprehensive approach to vehicle design and manufacturing aluminum, SAE, Technical Paper 870146, 1987.

Williams, N. T. Suggested topics for Future Research in Resistance Welding. Welding in the World 22 (1/2), pp. 28-34, 1984.

ABBREVIATIONS

AA : Aluminum Alloy
EDS : Energy Dispersive Spectroscopy
HAZ : Heat Affected Zone
HV : Hardness Vickers
LOM : Light Optical Microscope
Ra : Arithmetic Mean Value of Roughness
rpm : Revolution Per Minute
RSW : Resistance Spot Welding
RWMA: Resistance Welder Manufacturers' Alliance
std : Standard Deviation
SE : Secondary Electron
SEI : Scanning Electron Images
SEM : Scanning Electron Microscope
SORPAS : Simulation and Optimization of Resistance Projection and Spot Welding
SWANTEC : Scientific Welding and Numerical Technology
WSS : Weld Schedule Specifications
wt-% : Weight Percentage

Table 1 Resistance spot welders Specifications

Specifications	Values	Specifications	Values
Controller	TE-180, 16 Functions	Max. welding Power	810 kVA
Supply Voltage	380 V	Nominal power at 50%	250 kVA
Frequency	50 Hz	Phases	1
Max. welding current	68 kA	Supply pressure	6.5 bar
Max. welding force	18.85 kN	Electrode force per 1 bar	3.14 kN
Throat depth	250 mm	Net weight	1000 kg
Water cooling	12 ℓ / min		

Table 2 Strip material specifications

Trade name	Thickness (mm)	Tensile (MPa)	Hardness (HV)	Nominal composition (wt-%)				
				Fe	Si	Mn	Others	Al
AA1050	0.6	105	30	0.255	0.173	0.021	0.051	99.5
AA1050	1.0	105	30	0.378	0.100	0.018	0.004	99.5
AA1050	1.5	127	45	0.350	0.070	0.010	0.070	99.5

Table 3 Experiments setup (factors and their associated values)

Sheet (mm)	Welding Energy input					
	Low		Medium		High	
	Cycles	Current (kA)	Cycles	Current (kA)	Cycles	Current (kA)
0.6	2	20	5	23	9	26
1.0	2	23	5	26	9	29
1.5	2	26	5	29	9	32
Electrode Force 1.85-2.45 kN						

Table 4 Surface roughness values

Sheet (mm)	As-Received		Pickling in NaOH		Glass-Blast	
	R_a (µm)	std.	R_a (µm)	std.	R_a (µm)	std.
0.6	o.287	0.046	0.339	0.011	2.650	0.115
1.0	0.300	0.051	0.385	0.037	4.703	0.987
1.5	0.238	0.039	0.411	0.028	3.230	0.453

Table 5 WSS of weld planning optimization SORPAS®

Sheet	As-Received (mm)			Pretreatment (mm)		
	0.6	**1.0**	**1.5**	**0.6**	**1.0**	**1.5**
Welding Current (kA)	23.9	26.27	31.64	22.87	24.58	27.26
Welding Time (cycles)	2	4	5	2	4	4
Electrode Force (kN)	1.16	1.44	1.78	1.04	1.44	1.49

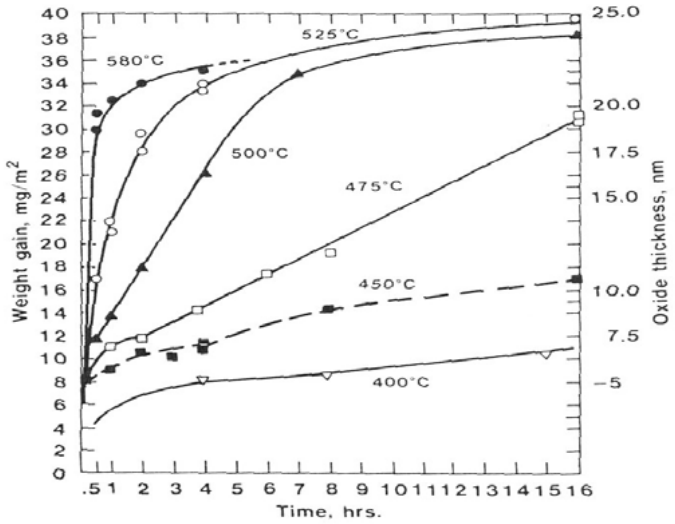

Fig. 1 Growth of oxide film for different temperatures [Pederson, 2010]

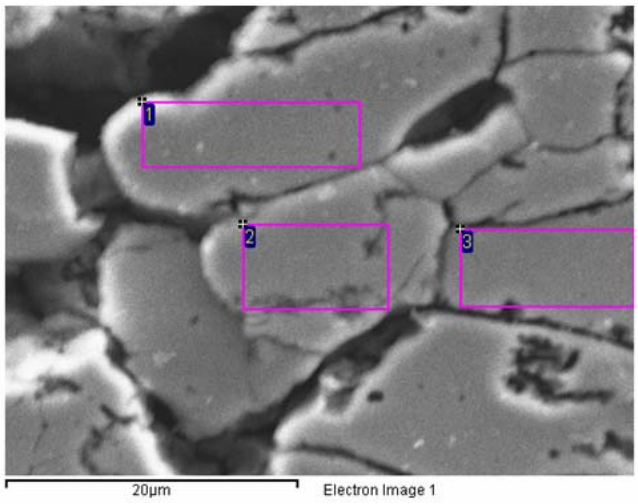

Processing option : All elements analysed (Normalised)

Spectrum	In stats.	O	Al	Total
1	Yes	3.6	96.4	100.0
2	Yes	4.6	95.4	100.0
3	Yes	2.9	97.1	100.0
Mean		3.7	96.3	100.0
Std. deviation		0.8	0.8	
Max.		4.6	97.1	
Min.		2.9	95.4	

All results in weight%

Fig. 2 SEM image and EDS analyzer for as-received spot-welded

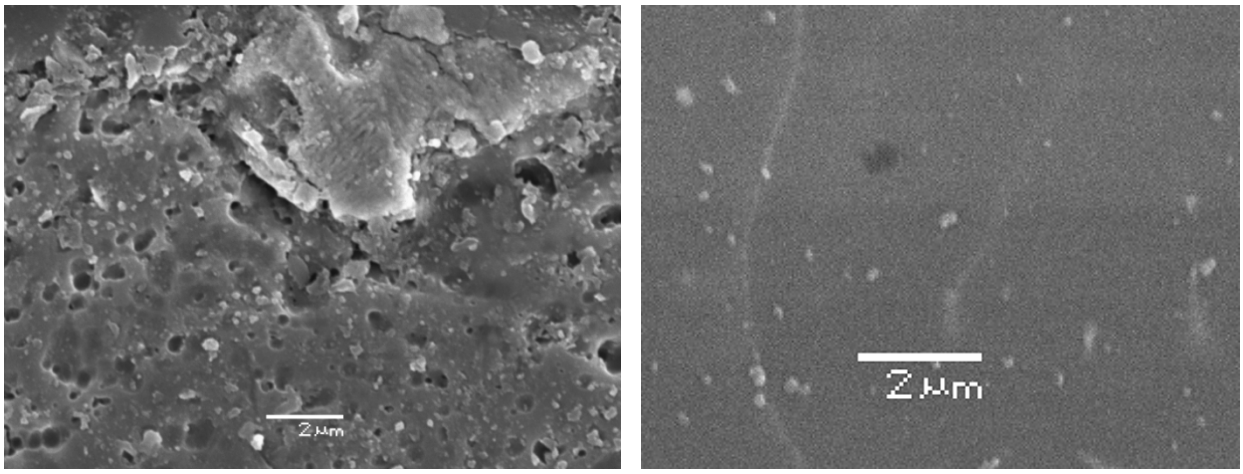

(a) **(b)**

Fig. 3 SEM images the sheets exposure to NaOH solution agent; **(a)** 1.0 mm within 5 minutes, **(b)** 1.5 mm sheet within 2 minutes

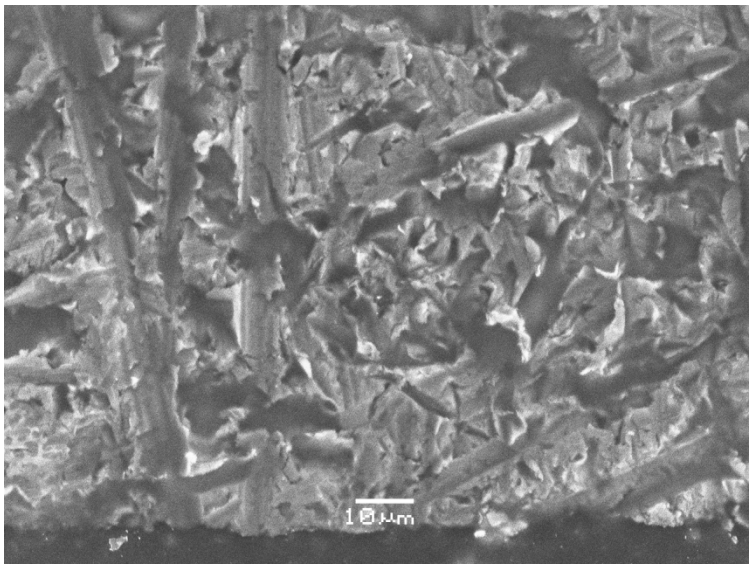

Fig. 4 SEM image RSW 1.0 mm glass blast sheet 29 kA, 5 cycles

Sheet	As-Received	Pickling in NaOH	Glass-Blast
0.6 (mm)	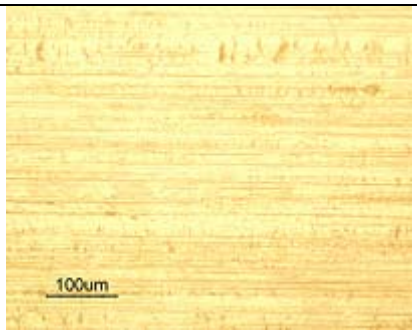	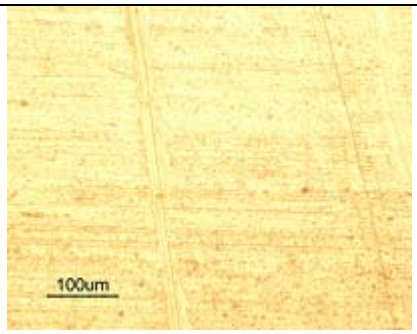	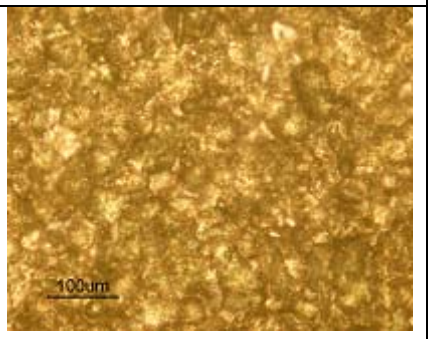
1.0 (mm)	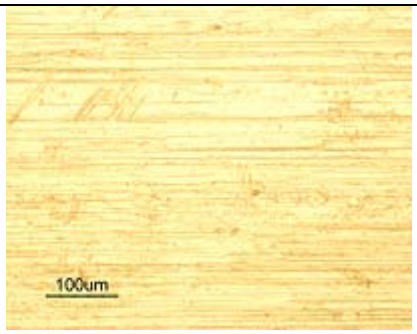	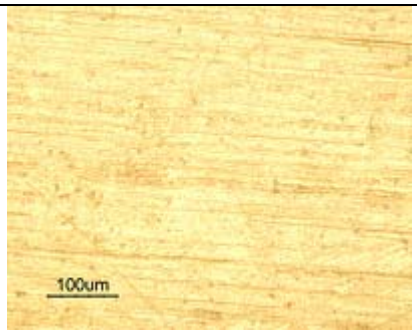	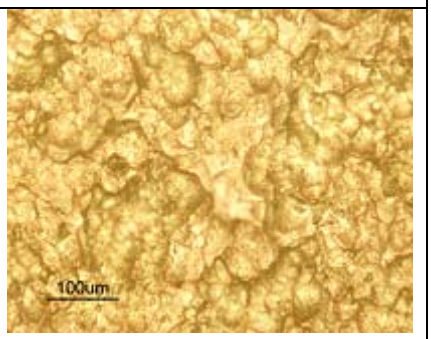

1.5 (mm)		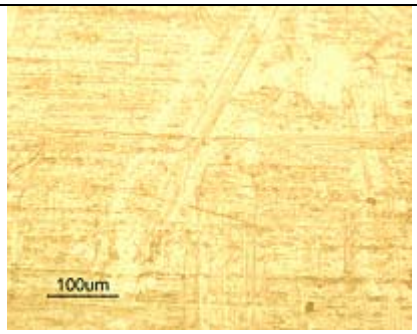	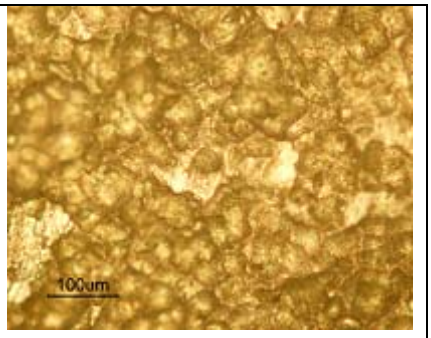

Fig. 5 LOM images, surface roughness of various type strips 200x

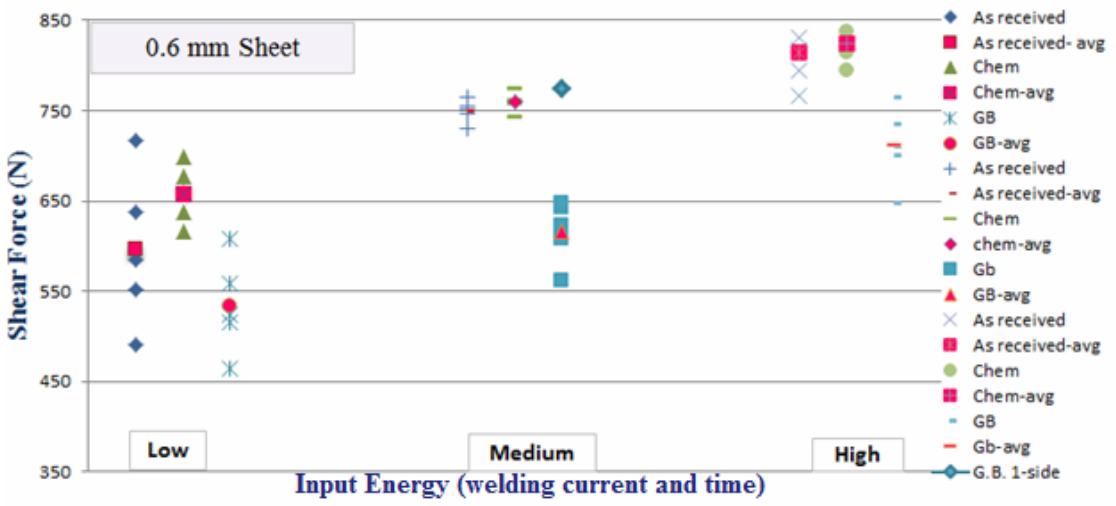

(**a**) 0.6 mm sheet

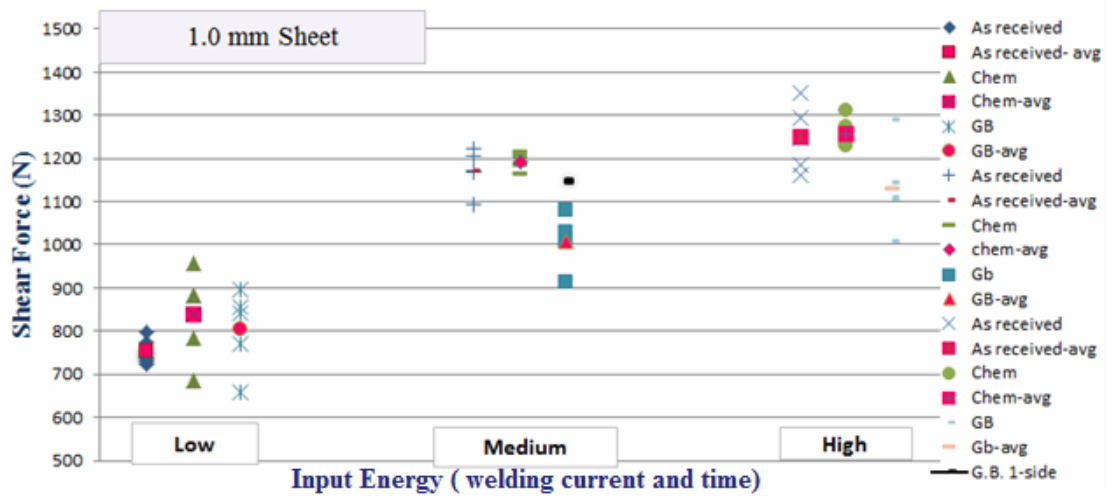

(**b**) 1.0 mm sheet

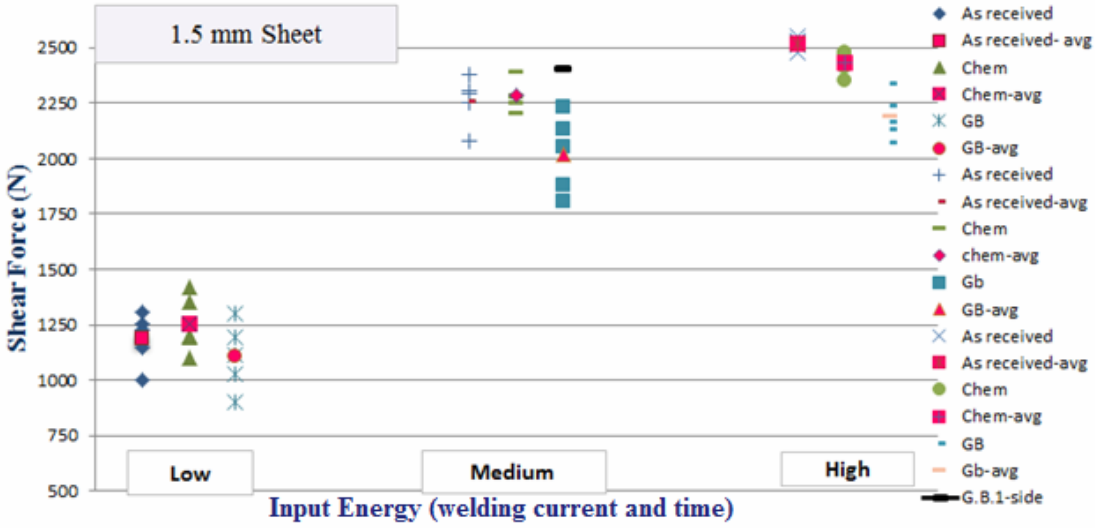

(**c**) 1.5 mm sheet

Key; avg: average, Chem: Chemical (Pickling in NaOH), GB: Glass blast

Fig. 6 Maximum fracture load versus the welding input energy in the tensile-shear tests

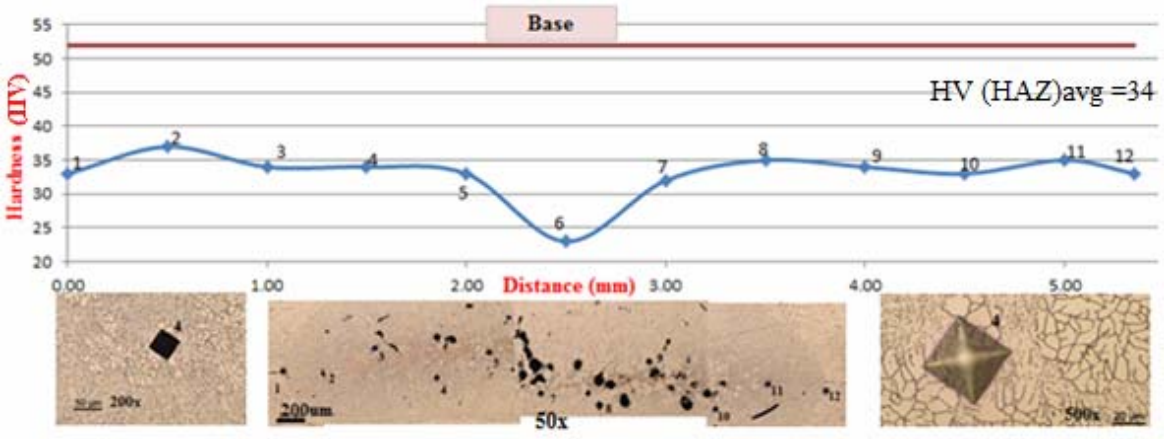

(**a**) Glass-blasted pretreatment surfaces

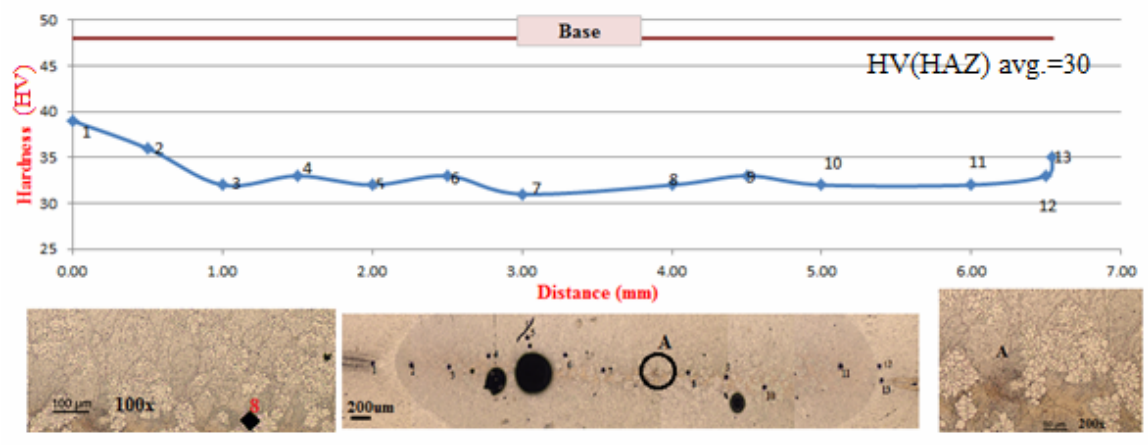

(**b**) Pickling in NaOH pretreatment surfaces

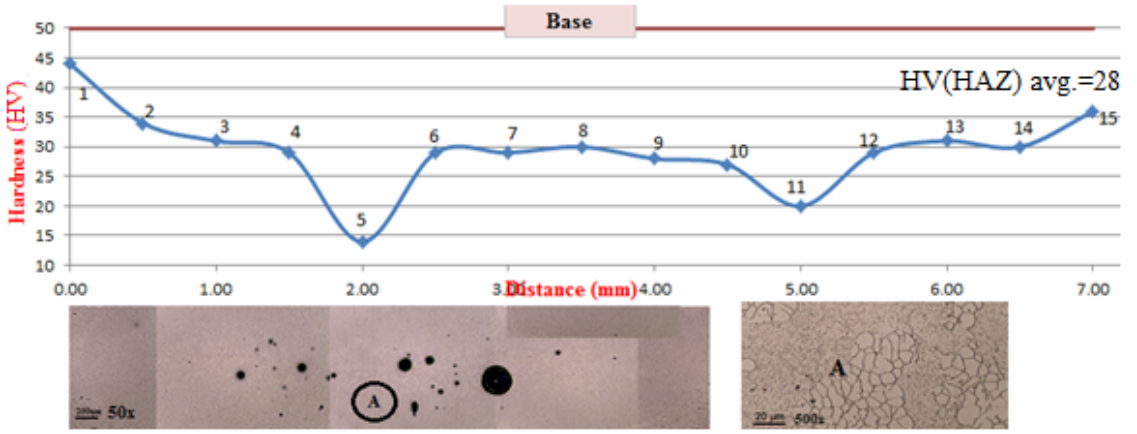

(**c**) As-Received sheet

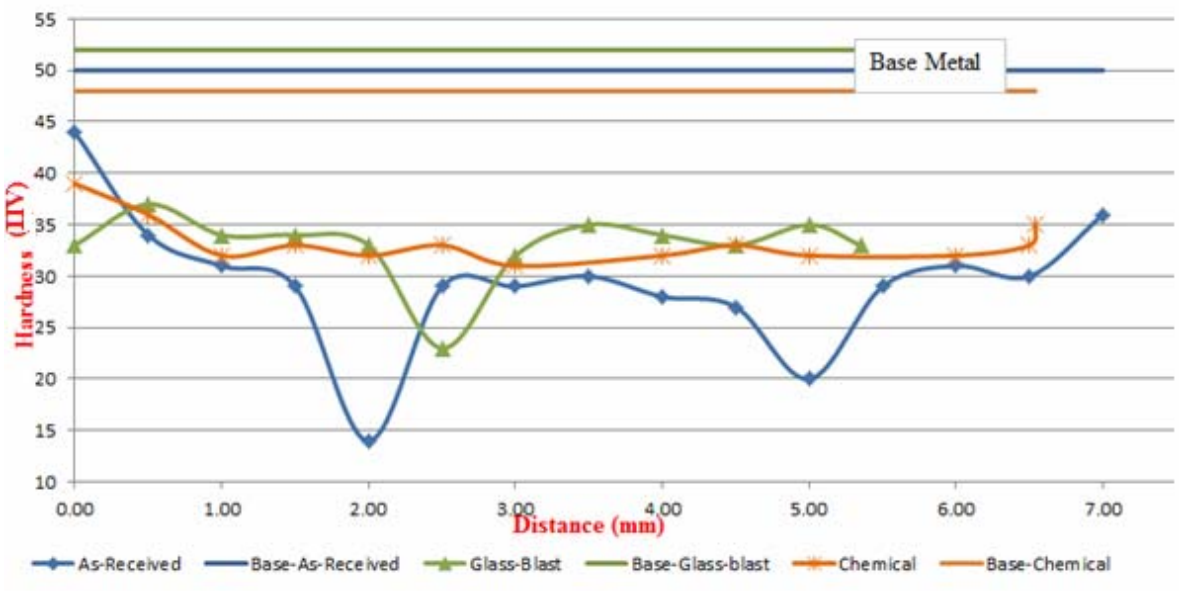

(**d**) All conditions sheets

Fig. 7 Microhardness profiles of 1.5 mm sheet, welding parameters (32 kA, 5 cycles)

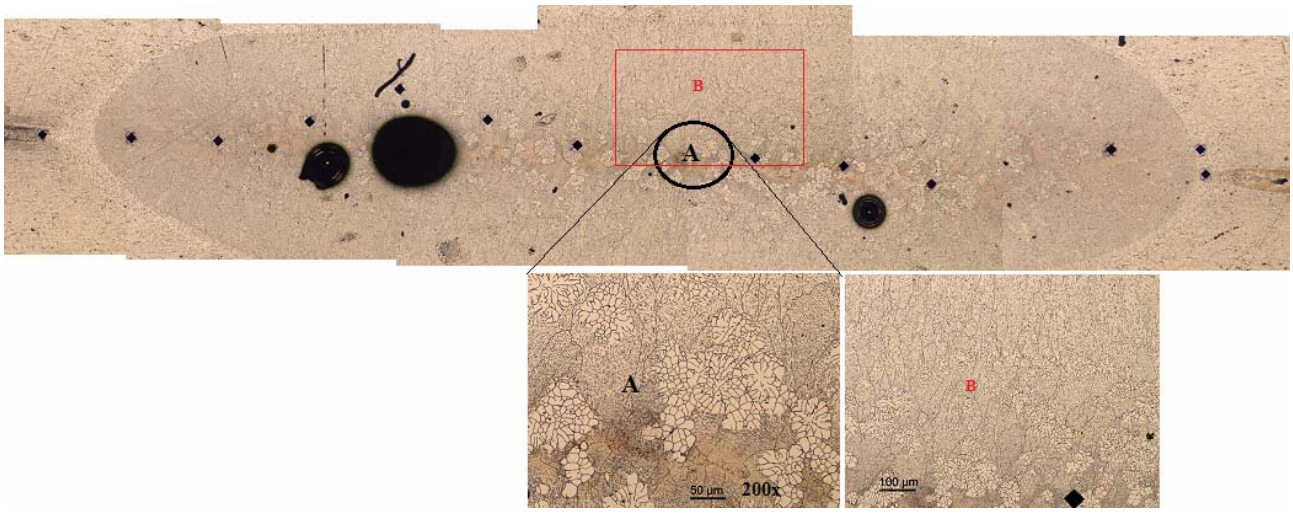

Fig. 8 Macro-Micrographs of RSW of 1.5 mm sheet, welding parameters (32 kA, 5 cycles)

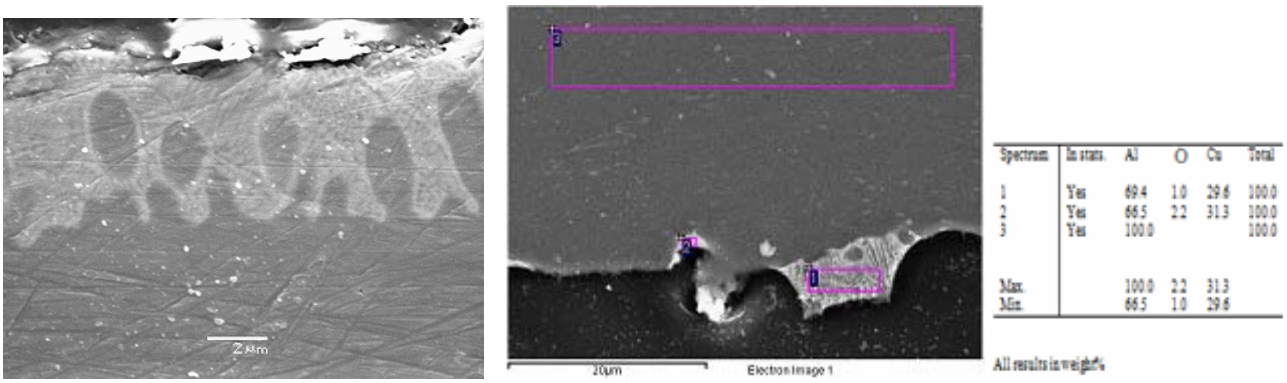

(**a**) 1.0 mm as-received sheet 8000x (**b**) 1.5 mm chemical pretreatment sheet 2700x

Fig. 9 SEM images RSW

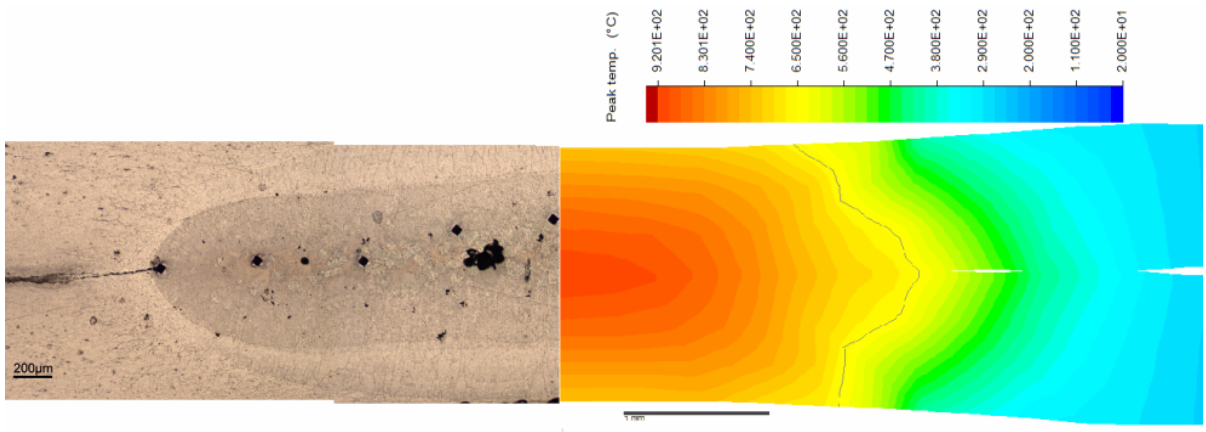

Fig 10 Comparison between SORPAS® simulation and a metallographic experimental result